# Colloidal Surface Assemblies: Nanotechnology Meets Bioinspiration

*Tobias Kraus, Daniel Brodoceanu, Nicolas Pazos-Perez, and Andreas Fery**

**This Feature Article discusses two biomimetic aspects of functional particle surface assembly: the fabrication of biologically inspired structures from particles and the arrangement of particles on biomimetic templates. The first part discusses the creation of primary patterns by convective assembly and adsorption of particles that can be modified by a combination of etching and growth steps. Resulting structures mimic moth eyes, Lotus leaves, and the Gecko's adhesive structures, for example. The second part focusses on template assisted self-assembly (TASA) of particles. Herein, biological examples are inspiring in terms of structure formation related processes, rather than in terms of functionality. Template formation is a major bottleneck TASA. It is illustrated how bio-inspired wrinkling processes help overcoming this problem and can be employed for forming highly ordered functional nanoparticle assemblies.**

## 1. Introduction

In this Feature Article, we discuss particle-based routes to microstructured surfaces. Many of these surfaces are inspired by naturally occuring structures. We also discuss structures that do not occur in nature, but can be fabricated using biologically inspired processes that involve particles.

Bioinspired functional surface microstructures often exhibit simple, more or less regular unit cells that are repeated over macroscopic length scales. The structures lead to functionality, for example (see **Figure 1**)

1. control of wetting, with the contact angles of liquid on the surfaces ranging from superhydropobic[1,2] and olephobic[3] to superhydrophilic,[4]
2. catalytic self-cleaning,[5]
3. reduced reflection of light,[6]
4. enhanced coupling of light out of[7] or into[8] an underlying active layer.

Dr. T. Kraus, Dr. D. Brodoceanu
INM-Leibniz Institute for New Materials
Structure Formation Group
Campus D2 2, 66123, Saarbrücken, Germany
Dr. N. Pazos-Perez, Prof. A. Fery
University of Bayreuth
Department of Physical Chemistry II
Universitätsstrasse 30, 95440, Bayreuth, Germany
E-mail: andreas.fery@uni-bayreuth.de

**DOI: 10.1002/adfm.201203885**

Small unit cells are sufficient because the functionality emerges at small length scales. They are set, for example, by the wavelength of electromagnetic radiation or by contact points between the functional surface and a liquid. Often, one or two length scales–usually the particle size and the spacing–dominates desired behavior. The unit cell is simply multiplied to create a macroscopic, "far-field" effect from this microscopic, "near-field" interaction.

It is possible to create such structures with conventional methods of microfabriction. However, the conventional combination of optical or electron beam lithography with silicon micromachining developed and perfected by the semiconductor industry in the last decades[9] is optimized to create arbitrary, planar structures from a very limited set of materials over small areas. It becomes expensive and complicated when used for three-dimensional sub-micron structures on large areas.

Moreover, functional surface microstructures rarely profit from the precision and flawlessness of bulk surface micromachining. Many functional microstructures tolerate deviations in geometry with only moderate loss in performance. If the unit cells function independently, flaws do not severely impede functionality, either: in contrast to semiconductor circuitry, where a single defective transistor may render the entire device useless, a Gecko will retain its adhesion to the wall when a microscopic spatula breaks of its feet. A biomimetic adhesion device does therefore not profit from a perfectly precise and flawless structuring technique. The effort required to reach this level of perfection is wasted.

In contrast, it is easy to create large quantities of sub-micron particles if some deviations from the average size are acceptable. Particles can be arranged on surfaces using efficient processes that do not yield flawless results but provide large patterned areas with little equipment.

Particles

- are easy to prepare in large quantities using simple setups once a protocol is established,[10]
- cover diameter ranges from single nanometers to hundreds of micrometers,
- can be composed of core materials suitable for microfabrication, including polymers,[11] metals[12,13] and oxides,[14,15]
- are well-established components of commercial surface coatings such as wall paint, finishes and protective coatings.

On the downside, particles usually exhibit

- some degree of distribution in size and shape over the population,
- a tendency to agglomerate into less well-defined objects,
- variations of the internal structure.

Most importantly, particles are randomly dispersed after synthesis. Assembly is required to arrange them into functional surface microstructures. If the desired microstructures have high aspect ratios (which are hard to create using particles), the particle arrangements can be processed further using standard micromachining techniques such as etching or deposition.

Particle assembly without templates only provides a limited set of arrangements—usually dense, hexagonal or loose, disordered packings. Such arrangements are useful for certain biomimetic applications: similar hexagonal particle packings can be the basis for antireflective and for superhydrophobic surfaces, for example, or combinations of both.[16,17]

Other particle arrangements require tuning of the assembly process with a template. Templated particle assembly provides a broad range of particle arrangements. If lithography is required to create the template, however, we lose some of the advantages of particle-based processing and again rely on demanding fabrication steps. Here, we review strategies to avoid this by

- combining template-less particle assemblies with particle adsorption, etching and deposition steps,
- assembling particles on biomimetic templates that can be created without microtechnology: wrinkles that form spontaneously (Figure 1).

In other words, surface microstructuring with particles can be biomimetic in two ways:

- by creating surfaces that imitate naturally occurring structures such that structure related functionalities are transferred (biomimetic function) and
- by using biomimetic structure formation processes to arrive at functional microstructures that may have no natural equivalent (biomimetic process)

The first approach is more familiar than the second. Most current examples of bioinspiration rely on dense particle packings to mimic similar, natural structures. Many useful, functional surface microstructures do not occur in nature, however. Others are only loosely inspired by biological counterparts, but deviate from the biological example in order to optimize their function in specific applications. Even for non-biomimetic structures, bioinspiration can be useful: natural structure formation inspires new fabrication schemes. Biological structure formation processes fundamentally differ from traditional technology. They do not require vacuum processes, have a modest thermal budget and consume less energy than standard technology. Biomimetic fabrication schemes exploit their principles to create functional microstructures efficiently.

The first part of this Feature Article discusses which biomimetic surface microstructures have been created from particles

**Prof. Andreas Fery** is chairholder of Physical Chemistry II at University Bayreuth and managing director of the Bayreuth Center for Colloid and Interface Science. His educational background is the University of Konstanz (M.Sc. Physics) and the Max-Planck Institute for Colloid and Interface Science/ University Potsdam, earning his PhD in 2000. His research interests are colloid- and polymer science with a focus on functional mesoscopic colloidal assemblies, responsive coatings/particles as well as surface patterning.

**Dr. Tobias Kraus** studied Chemical Engineering at the Technical University Munich in Germany, the Massachusetts Institute of Technology in Cambridge, USA, and the University of Neuchâtel in Switzerland. He obtained his PhD in materials science in 2007 in the group of Prof. Nicholas D. Spencer at ETH Zurich, Switzerland. His thesis discusses assembly mechanisms of particles, their transfer between surfaces and their application in technology. He collaborated with the IBM Research Laboratory in Rüschlikon, Switzerland, and subsequently joined it as a postdostoral fellow. Today, he heads the Structure Formation Group at INM and studies the behavior and application of particles in the synthesis of new materials.

**Dr. Nicolas Pazos-Perez** is currently a Postdoctoral Research associate of the Physical Chemistry II Department at the University of Bayreuth. He has a M.Sc. in Chemistry from the University of Vigo (UVigo, Spain) and received his PhD degree in Physical Chemistry in 2008 from the UVigo in collaboration with the Center of Advanced Studies and Research (caesar) in Bonn (Germany). His current interests focus on the wet chemical synthesis of plasmonic nanostructures, their surface modification and assemblies into 1, 2 and 3D nano and macro structures in order to control the inter nanoparticle coupling and collective behavior for sensing applications.

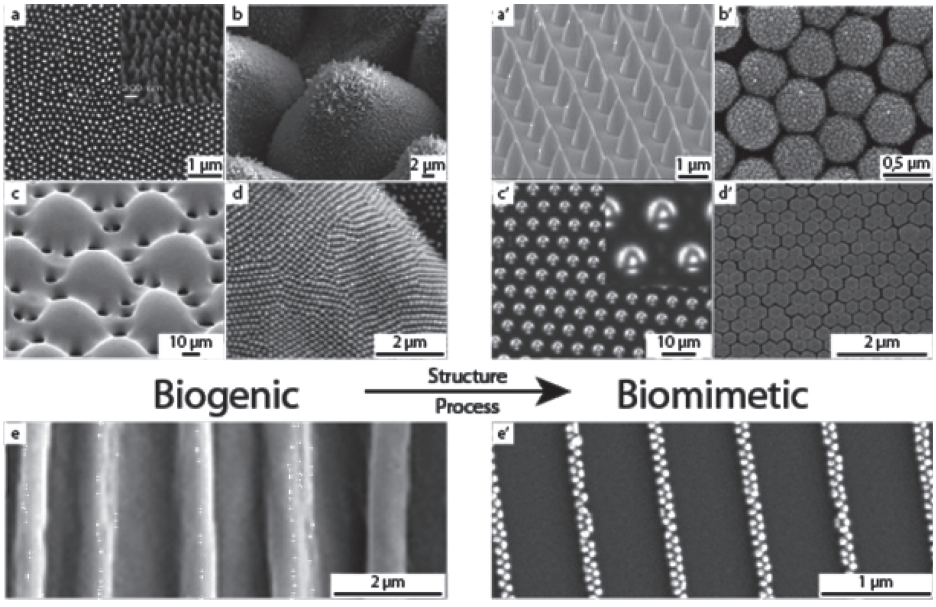


**Figure 1.** Structures found on surfaces of plants and animals (left side) and biomimetic, particle-based microstructures (right side). Natural inspiration is based, for example, on the surface microstructures of a) the antireflective wings of the cicada *Cryptympanaatrata Fabricius*. Reproduced with permission.[188] Copyright 2006, WILEY-VCH; b) The superhydrophobic leave of the taro *Colocasiaesculenta*. Reproduced with permission.[189] Copyright 2011, ELSEVIER; c) lenses in the peripheral layer of the dorsal arm plate of the brittle star *Ophiocomawendtii*. Reproduced with permission.[190] Copyright 2001, Macmillan Magazines Ltd; and d) the optically grated corneal nipple arrays of the peacock butterfly *Inachisio*. Reproduced with permission.[191] Copyright 2005, The Royal Society. Particle-based biomimetic microstructures include a') antireflective silicon cone arrays. Reproduced with permission[6] Copyright 2009, American Chemical Society; b') superhydrophobic, raspberry-like arrangements. Reproduced with permission.[2] Copyright 2007, American Chemical Society; c') microlenses from calcium carbonate (that show the magnified letter "A" here). Reproduced with permission.[192] Copyright 2012, Macmillan Publishers Limited; and d') superhydrophilic, self-cleaning titania nanocolumns. Reproduced with permission.[5] Copyright 2008, American Chemical Society. The wrinkles of the *Paeoniaceae* shown in (e) (reproduced with permission.[193] Copyright 2012, Published by The Company of Biologists Ltd) have inspired an assembly process for nanoparticles that yields lines as shown in e').Adapted with permission.[137] Copyright 2010, The Royal Society of Chemistry.

without using templates. It focuses on the convective assembly and sequential adsorption of particles to create primary patterns. We discuss how standard fabrication steps have been combined with the resulting particle arrangements to create biomimetic structures and which structures may be accessible in the future.

The second part focuses on functional surface microstructures that have been created using biomimetic wrinkles as templates. We introduce the principles of wrinkle formation as they also occur in nature, discuss how the resulting wrinkles can be used to arrange particles and which functional microstructures have been created on this route.

The field of biomimetic surface microstructures based on particles is young. Only comparatively simple structures have been created. In the final part, we discuss how more complex structures can be fabricated in the future using multi-level wrinkles and advanced particles that interact in complex, well-defined ways.

## 2. Particle-Based Routes to Biomimetic Structures

The fabrication of biomimetic surfaces requires reliable routes for nanometer-scale patterning of large areas with reasonable effort. During the last decade, colloidal lithography has emerged as a promising technology capable of generating ordered arrays of diverse features at scales often smaller than standard photolithography can achieve. Different colloidal lithography routes have been suggested to address the needs of a broad range of applications such as antireflective coatings,[18,19] self-cleaning surfaces,[20,21] biomolecular detection by surface-enhanced Raman scattering (SERS),[22] catalytic surfaces,[23,24] biomaterials[25] and other powerful templates for surface nanostructuring.[26,27] The strategy exploits self-assembled spherical particles with diameters ranging from several microns down to few tens of nanometers and represents a promising alternative to standard fabrication technologies, especially where periodic nanometer-sized features need to be scaled-up and where few defects do not affect the overall characteristics and function of the achieved structure.

There are several methods to generate self-assembled layers of hexagonally close-packed (hcp) particle arrays, such as dip coating,[28,29] spin coating,[30,31] electrophoretic deposition,[32,33] assembly at air/liquid[34,35] and liquid/liquid[36] interface, as well as convective assembly.[37,38] The latter permits fabrication of two-dimensional hcp arrays with fewer crystal defects due to a better control of the self-assembly deposition process.[39,40]

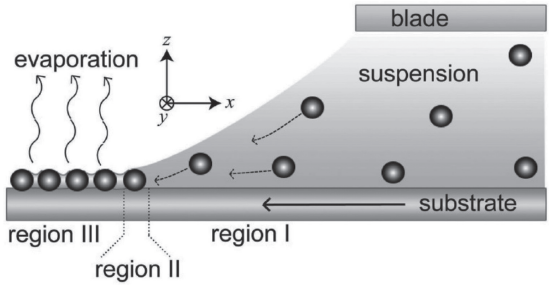


**Figure 2.** The three regions of convective particle assembly: In region I, the meniscus, free particles are convectively transported to the particle film. In region II, the particles are arranged to the particle film structure. In region III, the particles form a wet particle film with pronounced evaporation. Reproduced with permission.[194] Copyright 2012, American Chemical Society.

**Figure 2** illustrates how a droplet of colloid suspension trapped between two plates is dragged with constant velocity over a substrate surface during which the particles are transported to the edge of the growing crystal, driven by the flux of the liquid compensating for the evaporation from the crystal surface. The process has the potential for scale-up to large areas and for long operation time by continuously injecting colloid suspension into the moving meniscus.

A classic approach of colloidal lithography template is using the monolayer as a shadow mask for standard physical deposition. After removing the colloidal mask, ordered quasi-triangular metal islands result which can be converted to dots by subsequent annealing treatment.[41]

Often, applications require non-close-packed (ncp) templates.[26,42] One common technique to achieve ncp monolayers use reactive ion etching (RIE) by which the polystyrene (PS) particles from hcp monolayer are etched to increase the spacing between particles.[43,44] The process allows for tuning the diameter of the etched particles by varying the plasma power and etching times. Following the plasma etching treatment, the long-range order of the resulted ncp particle layer is preserved, provided that parameter optimization or additional treatments are performed.[45,46] Li and co-workers proposed an unconventional method for generating a spaced particle array by exposing the hcp PS monolayer to electron irradiation and subsequent annealing treatment.[47] Another efficient route to ncp particles arrays uses core-shell particles which consist of a core metal nanoparticle (NP) surrounded by a polymer shell. They can be deposited as hcp monolayers by convective assembly on virtually any smooth surface. Their shells are then thermally decomposed or plasma etched, leaving the metal NP cores in a regular hexagonal array (**Figure 3**d).[48,49] A slightly different approach was described in recent work by one of us,[50] in which the fabrication of metal nanoparticle arrays was achieved by controlled decomposition of polymer particles. Polymer spheres with submicrometer diameters were convectively assembled into crystalline monolayers, coated with noble metal and annealed in a resistive furnace or using an ethanol flame. The thermal decomposition of the polymer microspheres converted the metal layer into particles arranged in hexagonal arrays that preserved the order of the original monolayer. Both the particle size and the interparticle distance were adjusted via the thickness of the metal coating and the sphere diameter, respectively. Isa and co-workers reported on a method for the deposition of ncp regular arrays using electrostatically charged colloidal nanoparticles self-assembled at liquid/liquid interface.[51] Both particle size and spacing were independently controlled within a large range by changing the area fraction of the particles injected at the interface (Figure 3a). An interesting approach by which individual micro-sized islands of close-packed monolayer can be controllably transferred to a substrate was proposed by Palla-Papavlu and co-workers.[52] The method relies on laser-induced-forward-transfer (LIFT) where the size of polystyrene bead pixels depends on the laser parameters. Kraus et al. developed a novel printing process that enables positioning individual particles of sub-100-nm in diameter with high placement accuracy (Figure 3c).[53] Such colloidal particle arrays often serve as templates for 3D material nanostructuring with periodic

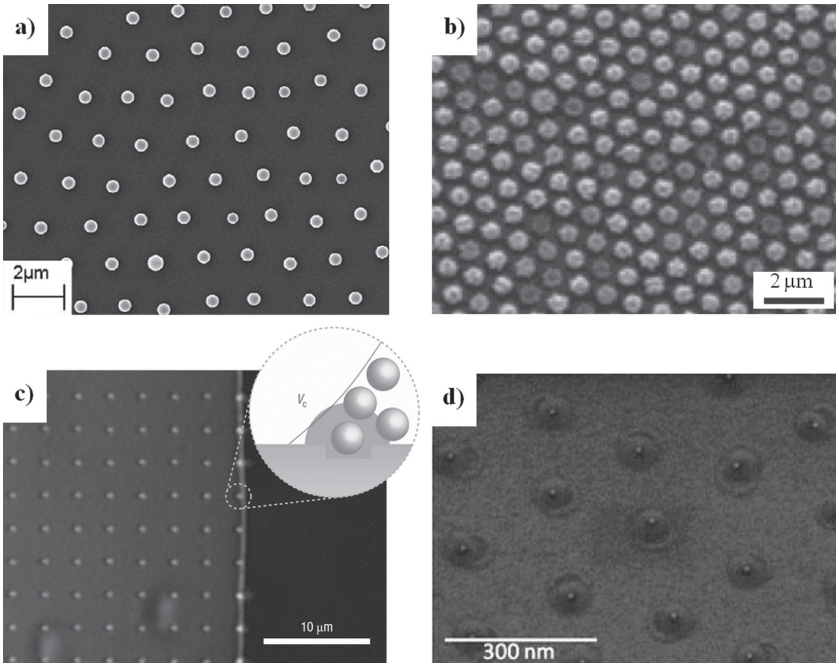


**Figure 3.** Examples of ncp arrays fabricated via different routes a) ncp polystyrene particles deposited on $SiO_2$ by colloidal self-assembly at liquid-liquid interface. Reproduced with permission.[51] Copyright 2010, American Chemical Society. b) Pattern produced by etching a polystyrene monolayer in $O_2$ RIE plasma. Reproduced with permission.[44] Copyright 2004, American Chemical Society. c) Particle Array formed by a meniscus of a colloidal suspension containing 60-nm Au particles moving over a patterned PDMS surface. Reproduced with permission.[53] Copyright 2007, Nature Publishing Group. d) Array of Pt nanoparticles fabricated by oxygen plasma treatment and thermal annealing of metal-complex containing latex particles. Reproduced with permission.[48] Copyright 2011, The Royal Society of Chemistry.

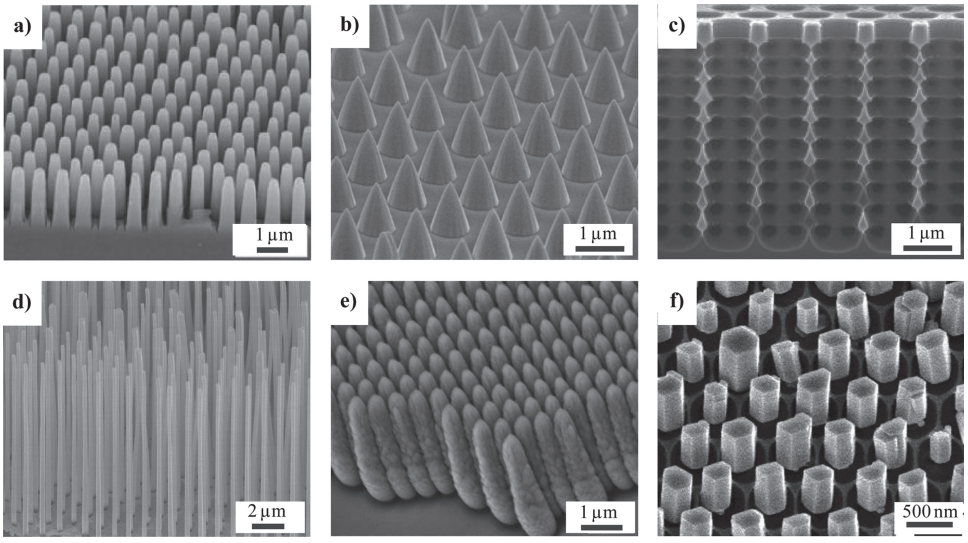


**Figure 4.** Three-dimensional structures from self-assembled particles and subsequent processes. a) Silicon pillars achieved via reacting ion etching (RIE). Reproduced with permission.[16] Copyright 2008, WILEY-VCH. b) Silicon cone array by RIE. Reproduced with permission.[6] Copyright 2009, American Chemical Society. c) Holes array fabricated by sequential passivation reactive ion etching (SPRIE). Reproduced with permission.[27] Copyright 2013, WILEY-VCH. d) Si nanowire array by metal-assisted chemical etching (MACE). Reproduced with permission.[26] Copyright 2007, WILEY-VCH. e) Nanopillar arrays grown by glancing angle deposition (GLAD). Reproduced with permission.[57] Copyright 2005, Elsevier. f) ZnO pillars grown using a wet chemical route. Reproduced with permission.[195] Copyright 2009, American Chemical Society.

nanofeatures. The patterns are transferred to substrates via specific routes which involve processes like reactive ion etching (RIE),[16,44] metal-assisted-chemical-etching (MACE),[26,54] electrochemical etching,[55] vapor-liquid-solid (VLS) growth,[56] grafting[57] or molding.[58] **Figure 4** shows examples of surfaces structured based on self-assembled particles used in combination with the aforementioned processes. Other routes based on controlled annealing of hcp PS layers,[59,60] ion milling[61] or Glancing Angle Deposition (GLAD)[57] allow for fabricating of novel patterns. Replicating methods use master templates to reproduce the original structures via molding.[58] With this approach, polymers such as polydimethylsiloxane (PDMS) can be rapidly nanostructured.[58,62,63] **Figure 5** illustrates an example of replicating route based on self-assembled particles.

Such particle-based methods have been successfully applied by many groups to fabricate bioinspired surfaces with antireflective[18,64] and superhydrophobic[2,65,66] properties. Antireflective coatings have technological applications, e.g., to increase the conversion efficiency for solar cells,[67] but also for anti-glare flat panel displays or automobile windshields. The nanometer-scale structure of the moth eye has inspired material scientists in their quest to build effective antireflective coatings. Close-up images of the moth eye reveal both the periodic nature and the main physical characteristics of its structure. To avoid light scattering, the structures need to be smaller than the wavelength of the incident light. Photolithography, e-beam lithography or focused ion beam have been used in the past for fabrication of these structures. Such methods, however, are expensive, challenging to scale-up and only suitable for flat substrates. In contrast, colloidal particle assembly overcomes these constraints and allows large-scale patterning with submicrometer features on both flat and curved substrates.

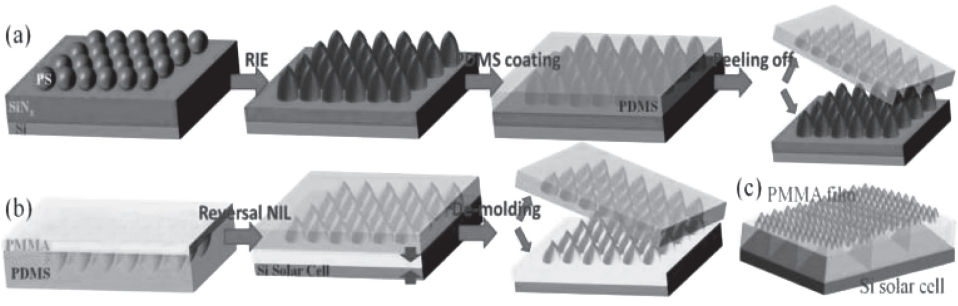


**Figure 5.** Schematics and flow chart of the biomimetic nanostructure making processes. a) Si mold fabrication using the colloidal lithography and duplication of the Si mold with PDMS; b) reversal nanoimprint lithography; and c) illustration of surface textured crystalline Si solar cell with nanostructured PMMA AR coating. Reproduced with permission.[58] Copyright 2011, Optical Society of America.

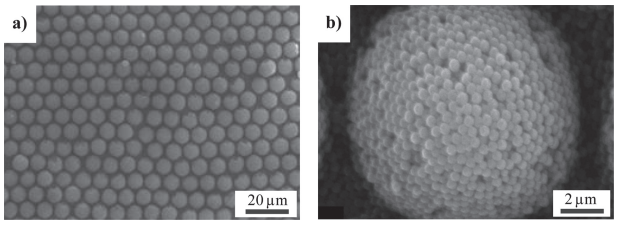


**Figure 6.** SEM images of dual-size-rough surface. a) Array of microspheres, each composed of 300 nm silica nanospheres; b) Close-up view of (a). Adapted with permission.[1] Copyright 2006, Elsevier.

Another famous example of a natural functional surface is represented by the lotus leaf, which exhibits remarkable hydrophobic properties. In contact to a lotus leaf surface, water droplets assume a nearly spherical shape.[68,69] A closer look at its surface reveals densely packed papillae with the diameter in the range of 3–10 µm, each of them decorated with nanometer-scale protrusions.[70,71] Inspired by this natural nanoarchitecture, researchers were able to fabricate functional materials with similar hydrophobic properties.[1,72] **Figure 6** shows SEM images of hexagonal packed microspheres composed of silica nanospheres with a diameter of 300 nm, achieved using a PDMS template with honeycomb structure.

Colloidal lithography holds great promise for realization of powerful hierarchical templates in silicon for molding polymers (e.g., PDMS) that is expected to mimic the nanostructure found on Gecko toes. The strategy relies on a sequence of technological steps, starting from ncp particles array defined by oxygen RIE followed by an etching process such us metal assisted etching or deep reacting ion etching to generate dense arrays of straight holes with aspect ratio ranging from 3 to 6. By stacking additional patterned layers of thick photoresist (SU-8), hierarchical templates can be fabricated which can be inverted and transferred into PDMS via molding.

## 3. Surface Microstructures from Particles Assembled on Biomimetic Wrinkled Surfaces

For many technical applications colloidal arrangements are considered promising building blocks for the realization of novel devices including sensors, waveguides or solar cells among others.[73] Therefore, great effort has been dedicated towards understanding and controlling particle assembly during the past years.[74–77]

One of the most successful approaches towards controlling particle assembly on surfaces is template assisted self-assembly. Here, particles are "guided" by chemically or topographically structured substrates. For instance, chemically prestructured substrates have been use to produce micropatterned photonic crystals.[78–80] Convective assembly as described in the first section of this article provides access to highly regular one- and two-dimensionally ordered particle arrays when structured templates are employed. Alternatively, Khanh et al. introduced dry assembly[81] obtaining quasi-two-dimensional colloidal arrangements which could further be used to direct particle assembly by colloidal epitaxy.[82–84] However, topographical templating introduced by Xia and co-workers.[85] is more common and allows organization of particles of different shapes with exceptional precision.[86–90] Often unusual crystal structures which differ from close-packed monolayers result from the prestructuring of the template.[85,91–95]

While template assisted self-assembly shows an impressive control over positional order and provides access to complex, almost arbitrary patterns covering several length scales, the main drawback is the need for specifically designed templates. These templates are usually produced by photolithography and if submicrometer dimensions should be approached, even more complex procedures like extreme UV interference lithography,[96,97] e-beam lithography (EBL)[98] or focused ion beam (FIB)[99] etching are required. The employed processes are rather expensive and energy consuming, especially when structuring in the submicron regime is required. Up-scaling is as well problematic especially for techniques which are locally invasive like EBL and FIB. While nanoimprint techniques simplify replication, they as well require first masters formed by the techniques mentioned above. Thus, template formation turns out to be a bottleneck for both fundamental research and applications of template assisted colloidal self-assembly. This is the main reason why template assisted self assembly approaches are generally seen as difficult to up-scale and of high complexity/cost.[74]

At this point, it is instructive to review surface patterns found on biological and especially plant surfaces, since they point towards a possible solution of this problem. As shown for the example of plant surfaces in **Figure 7**, natural surfaces display an abundance of various topographical patterns. Patterns often display periodical lines-features with periodicities down to micron dimensions. In many cases, the underlying structure forming process for these so-called cuticullar folds is wrinkling, which is a general mechanical instability phenomenon: surfaces composed of an elastic layer and a stiffer top coating start to buckle forming periodic sinusoidal structures upon application of mechanical strain.[100] This process is of course not limited to biological interfaces, but is as well found on various artificial surfaces.[101,102]

The physics of wrinkling processes has been investigated in great detail (see Ref. [103]). Wrinkling phenomena are based on so-called buckling instabilities of thin films[100,104,105] meaning that when a compressive in-plane strain is applied to a thin membrane it will respond with low deformations. It will bend out of plane developing a wrinkle, as frequently observed for cloth, skin, or paper. Although the formed wavelengths of a free sheet are generally scattered over a broad range, the situation changes as the sheet is coupled to an elastomeric substrate. In this situation, wrinkle-wavelengths become well-defined and can be used for templating.[106]

Biot and Landau[107–109] developed the buckling mechanics which Voliinsky et al.[110] used for the study of this phenomenon. The basic underlying principle is that there are—in contrast to the free sheet situation—two main contributions towards the total mechanical deformation energy of the system. One is related to the deformation of the thin sheet, as in the free sheet scenario. This contribution is minimal if sheet bending is low and thus favors large wavelengths. The other contribution is related to the deformation of the substrate and

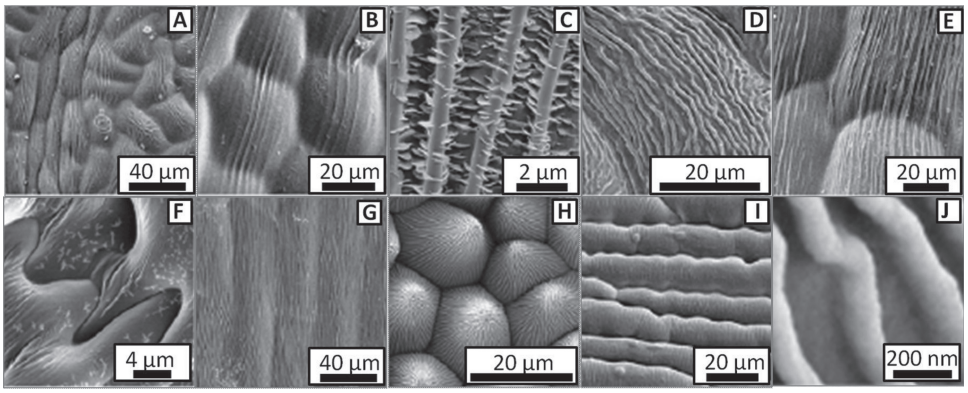


**Figure 7.** Cryo-scanning electron microscopy (cryo-SEM) micrographs of cuticle folds on plant surfaces. A) Upper (adaxial) leaf surface of "*Malus domestica Borkh*" (Rosaceae). B) Main vein on the lower (abaxial) leaf side of "*Rumex obtusifolius L*" (Polygonaceae). C) Lower leaf surface of "Polygonatum multiflorum (L.) All." (Asparagaceae). D) Upper leaf side of "Rheum rhabarbarum L." (Polygonaceae). E) Stem of "Rheum rhabarbarum L." (Polygonaceae). F) Lower leaf side of "Solanum tamii Hawkes and Hjert" (Solanaceae). G) Upper flower surface (petals) of "Paeonia Hybr." (Paeoniaceae). H,J) Upper flower surface (petals) of "cardamine pratensis L." (Brassicaceae). I) Upper flower surface (petals) of "Taraxacum officinale L." (Asteraceae). Adapted with permission.[193] Copyright 2012, The Company of Biologists Ltd.

favors minimal amplitude of the sheet deformation, which corresponds to minimal wavelength at fixed relative deformation. The sum of both contributions becomes minimal at a finite wavelength, defining preferred periodicity.

Continuum mechanical considerations quantify the important parameters and their relation to geometrical and mechanical quantities: A critical relative deformation $\varepsilon_c$(Equation (1)) is required to observe wrinkling where $E_f$ and $E_s$ are the Young's moduli and $\nu_f$ and $\nu_s$ the Poisson's ratio of the film and the substrate, respectively. The wavelength ($\lambda_c$) (Equation (2)) and amplitude (A) (Equation (3)), are directly related to the thickness of the film ($h_f$).

$$\varepsilon_c \left( \frac{9(1-\nu_f^2)^2 E_S^2}{64(1-\nu_S^2)^2 E_f^2} \right)^{\frac{1}{3}} \tag{1}$$

$$\lambda_c = 2\pi h_f \left( \frac{(1-\nu_S^2)E_f}{3(1-\nu_f^2)E_S} \right)^{\frac{1}{3}} \tag{2}$$

$$A_0 = h_f \left( \frac{\varepsilon}{\varepsilon_c} - 1 \right)^{\frac{1}{2}} \tag{3}$$

However, these equations are only valid for low values of the strain ($\varepsilon_c$). Huang and Jiang et al.[111,112] studied the influence of high stresses on thin film buckling. They found that the wavelength decreases for higher strains as shown in Equation (4) and Equation (5).

$$\lambda[A] = \frac{\lambda_c[A_0]}{(1+\varepsilon)^{\frac{1}{2}}(1+\xi)^{\frac{1}{3}}} \tag{4}$$

$$\xi = \frac{5\varepsilon(1+\varepsilon)}{32} \tag{5}$$

The fact that topographical features of wrinkling patterns like periodicity and amplitude become well-defined and controllable by film thickness and elastic properties of film and substrate opens a (bio-inspired) route towards topographical patterning: wrinkling has consequently been exploited for topographical structuring of artificial systems. The first example was reported by Whitesides et al.,[101] who deposited a thin metal layer on a thermally expanded elastomeric polymer. Due to the contraction of the underlying elastomer upon cooling, periodic wrinkles with wavelengths of 20–50 µm were formed. Due to the isotropic expansion of the elastomer, the wrinkles formed vermiculate patterns with no preferred orientation. Both the missing long range orientation and the rather large periodicities have been massively improved by alternate approaches.

If the isotropic stress is replaced by a uni-axial mechanical stress, parallel macroscopically oriented wrinkles are formed upon relaxation. Thus wrinkle orientation becomes well-defined on macroscopic areas. As the underlying mechanism is based on mechanical deformation properties and geometrical features, the process can easily be generalized to a wide variety of other material-combinations. In particular, while PDMS is by far the most widely used substrate, the nature of the thin film was varied by many groups: for instance using various polymers films,[113–117] polymer brushes[118] or thin oxide layers prepared by oxidation either with plasma,[119] UV–ozone[120] or via chemical treatment,[121] leading to various structure types and wrinkle dimensions.[100,106,122–124] In terms of periodicities, plasma oxidation of PDMS is most widely used for approaching the low-wavelength limit. Periodicities of 300 nm and less have been reported in the literature.[106]

Additionally, wrinkles based on elastomeric systems can be used as a mold to transfer the well-defined structure on substrates with various surface chemistries, which was first introduced by Schweikart and co-workers.[125] The approach was recently expanded to templating of inorganic materials.[126] Replication may increase the stability of the surface against solvents and mechanical impacts, which broadens the applicability of surface wrinkles.

If one compares wrinkle type structures to structures formed by lithography, one major difference is the nature of defects

that occur in the process. In lithographic techniques, patterning arises due to the fact that part of a substrate is removed by etching. Ideally the transition between etched and non-etched regions is infinitely sharp, in reality it has a finite width and roughness, which is determined by processing parameters. The aim of process optimization is to reduce these non-idealities. In contrast, structure formation based on wrinkling is not a locally invasive process. Rather, mechanical response towards a macroscopic deformation causes the morphological changes. Defects can arise from mechanical failure, mechanical inhomogeneities, but they can as well be a consequence of metastable states in mechanical deformation energies. Defects that are caused by mechanical failure are, for example, cracks which are frequently observed in cases where brittle layers are used for wrinkling. Efimenko and coworkers,[127] reported crack formation in samples of PDMS covered with a layer of silica-like material, which were uniaxially strained. Cracks were oriented perpendicular to the wrinkle direction and could be explained by transverse deformation. Similar effects are frequently encountered. In many cases, they pose no fundamental problem, since they occur at typical distances much larger than the wavelength of the wrinkles. If cracks should be avoided, more elastic layers have to be used for wrinkling. For example Chen and coworkers report on a crack-free controlled wrinkling method, based on a bilayer film system with a vertical gradient in material stiffness.[128] The observed reduction of crack formation and delamination are caused by a reduced stress intensity factor of the system which results in increased resistance of the system to structural failures. However, cracks can as well be used for adding complexity/additional levels of hierarchy to wrinkle patterns. For example, Crosby and co-workers illustrated that cracks can serve as ordering elements for wrinkles.[129,130] The second class of defects are minutiae, "Y"-type junctions of wrinkles. As in human finger-prints, minutiae occur at random positions. The density of minutiae depends on the mechanical homogeneity of the system and on the process of wrinkle formation. Even if a system is mechanically perfectly homogenous, minutiae can form as metastable states.[131] Again, they can serve as interesting symmetry breaking elements, which will be further discussed in the final part of this section.

An important consequence of both defect mechanisms is that long range order is very difficult to achieve using a wrinkling approach in contrast to lithographic techniques. Lithography defects are not disturbing long range order, since they are local and not "additive", cracks or minutiae disturb long range order. Thus, wrinkling is most attractive for applications, where only local order is required—such as optical effects—while it is ill-suited for "high definition patterning" as is required in data storage applications. This already defines a first scope of possible applications. In the following section, we will focus on the application of wrinkles as templates for particle assembly. However, there is a broad range of other possible applications of wrinkles related to other surface aspects like optical properties, friction, adhesion, etc. which are covered by recent reviews.[132–134]

There are many examples in particle-based microstructuring, where micrometer- or even sub-micrometer periodicities, but no extreme long range order are desired such as optical bandgap or plasmonic coupling.[135–138] The first use of wrinkled surfaces for particle alignment and formation of periodic structures was presented by Lu et al.[139] In this proof-of principle, particles were deposited onto a wrinkled surface by dip coating. This process has been demonstrated in the following to be very versatile in terms of particle type used by Hyun et al.[140] However, dip coating has limitations in terms of up-scalability. Spin coating has been shown to be an alternative. During the rotation cavities are filled with particles and the excess are spun away by centrifugal forces.[141–143]

Schweikart et al. showed that particle suspensions can be ordered by confinement between a flat substrate and wrinkles. In this confined state the particles are trapped in the formed microchannels during drying. One advantage of this approach is that the organized particles are directly transferred to the used substrate after removing the wrinkles. Another advantage of this approach is that different structures can be achieved, ranging from single lines, double lines to pyramidal like assemblies by tuning particle concentration and wrinkles wavelength. Additionally, grid like structures can be also achieved by confining the particle solution between two wrinkled surfaces.[106,123,144,145] An improvement on particle organization using wrinkles was developed by Fery and co-workers using a combination of these two last approaches (spin coating and confinement; see **Figure 8**). In this technique, the spin coated particles fill the cavities of the wrinkles and are further release to glass slides under confined conditions using a water droplet.[145,146]

Wrinkling does not only provide an access towards topographical templates, as well, wrinkle patterns can be translated into chemical patterns as introduced by Pretzl et al.[147] In this work, wrinkled elastomers were used as microcontact printing stamps and polymers could be patterned with sub-microometer periodicities. Similar microcontact printing approaches were subsequently used by many authors for transferring particles

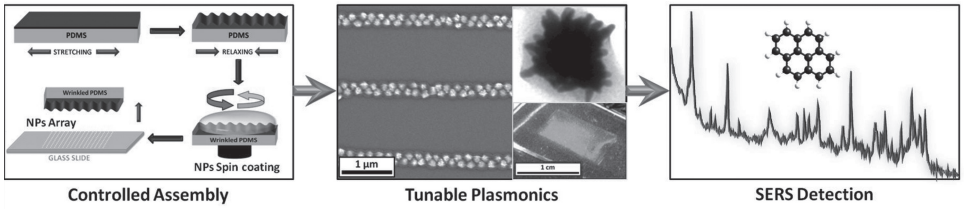


**Figure 8.** Schematic representation of the spin coating and confinement combination approach to organize particles (left). SEM, TEM and digital picture images showing gold stars coated with PNIPAM organized into parallel lines (center). SERS spectrum of pyrene showing the ability of this structure for sensing (right). Reproduced with permission. [146] Copyright 2012, American Chemical Society.

assembled in wrinkles onto other substrates.[141–146] An interesting alternative is the printing process introduced by Hyun and co-workers, which have shown that wrinkles made of PS coated PDMS can be reversible buckled by thermal recovery, due to induced buckling by strain and release by glass transition of PS layer. Therefore, the deposited particles can be easily transferred to other substrates by undergoing the buckled to flat transfer.

Mostly spherical colloidal particles, like silica[148,149] or PS[139,140,144,149] have been aligned. However, not only spherical or inorganic particles can be organized. Efinmenko et al.[149] and Horn et al.[141] showed respectively, that also life entities like zoospores or tobacco mosaic virus with anisotropic morphology, can be organized using wrinkles. Besides particle organizations, wrinkles have been demonstrate to be useful for other particle applications as Efinmenko et al. demonstrated the use of wrinkles as microfluidic sieves using two different periodicities.[127]

In contrast to "classical" template assisted particle assembly schemes, two facts make wrinkle assisted assembly very attractive. First, the process appears to be robust enough to work well for sub-micrometer particles, for which many alternate approaches as reported by Velev fail.[74] Using wrinkle-substrates as templates, assembly of sub-micrometer particles is routinously reported. For example Lu and co-workers used polystyrene particles of 380 nm,[139] Mueller and co-workers used 250 nm Au@PNIPAM (poly-N-isopropylacrylamide) particles,[146] or Pazos-Perez et al. used 66 nm gold particles[137] Second, the assemblies can easily approach macroscopic areas while maintaining nanoscale control on particle order and distances between particles (see Figure 8). These two aspects are of particular relevance for technological applications: the organization of nanoparticles into ordered or even hierarchical structures is one of the current challenges in nanotechnology. Many novel electronic, optic, mechanic or magnetic properties arise only in such assemblies where interparticle coupling or long range cooperative behavior can be tailored by a controlled short and/or long range order. Typical examples are structures with metamaterial properties or controlled plasmonic properties.[150–159]

Regarding this aim, various functional particles had been used to produce periodic organized structures. One of the most used particles are metallic nanoparticles because of their interesting optical properties which are the focus of interest in controlling interparticle surface plasmon coupling. Organized surfaces of Au NP using wrinkled substrates, had been mainly performed either via printing,[140] dry confinement,[137,144] or spin release.[145]

In this context, particle organization has not been only restricted to hard particles. Also soft colloids like thermoresponsive microgels had been organized as shown by Hyun et al.[140] Keeping in mind the applicability of these structures, the use of core shell particles where the cores provide functionality, Mueller et al.[145] used silver and gold NP as cores with PNIPAM shells showing that the soft shell acts not only as spacer, thus controlling plasmon coupling by tuning the interparticle distance, but gives also the opportunity to build up new packing geometries of the particles within a line moving away from closed packed structures due to the fact that the shell is soft and can be easily deformed during the spin release. Therefore, not only the angle between particles is distorted, but also the distance between them can be decreased.

Currently, one of the most promising technological applications of these systems which arise from controlling plasmonic coupling is the generation of high electromagnetic fields in confinement regions[160–165] that can be used to enhance different material properties or to induce new metamaterial properties. Surface enhanced Raman scattering (SERS) spectroscopy, is widely used at the moment because is a powerful ultrasensitive and very fast technique which allows detection down to single molecule levels.[166,167] The production of active SERS substrates is based on the generation of hot spots created by plasmonic nanoparticles. However, the controlled formation and reproduction of these hot spots is still a challenge in order to produce homogeneous and reproducible SERS intensities over large areas. This is a requirement in order to go one step forward to overcome the restricted qualitative results of this technique toward quantitative and reproducible measurements.

To this end, Pazos et al.[123,137,168] used the wrinkle assisted assembly process in order to organize gold nanoparticles into parallel lines and thus generating an homogenous array of hot spots at the gaps between particles, demonstrating the homogenous intensity provided by the substrate over large areas. Moreover, one of the most prominent plasmonic structures for SERS analysis are star shaped nanoparticles[169] which actually exhibit numerous hot spots within a single nanoparticle at the apexes of the tips[170] being one of the first substrates providing Raman enhancement at the single-particle level.[171] However, it has been shown that close packed arrangements of these structures results in deactivation of the hot spots due to the interaction between tips with different geometry and orientation, giving rise to plasmon deactivation rather than to the generation of highly active hot spots, as in the case of spheres.[172,173] To address this problem, Mueller et al. used aligned gold stars with a PNIPAM shell in order create extended homogeneous periodic structures avoiding tip to tip interactions and thus preserving the full SERS activity of each nanostar.[146] Additionally, a second functionality of these assemblies was demonstrated by using the hydrophobic nature of the PNIPAM shell to trap and detect aromatic hydrocarbons (pyrene) in gas phase as shown in Figure 8.

Concerning future developments of this approach, the step from simple patterns and symmetries like parallel lines to hierarchical patterns is probably the most exciting perspective. Again the natural examples demonstrate impressively that wrinkling is suitable for achieving highly complex hierarchical patterns (see Figure 1). Artificial wrinkling is beginning to follow this inspiration, using different strategies, which will be reviewed in this section.

There are many examples of wrinkle structures which deviate from parallel line-morphology reported in literature as for instance random, herringbone,[174–176] stripes,[101,110,115,119] checkerboard,[177] and others discussed in several rev iews.[100,106,178] However, to generate hierarchically[177–185] structured surface patterns of high quality, with high reproducibility and controlled surface properties is still a challenge in materials science. In this context, the wrinkling methods remain

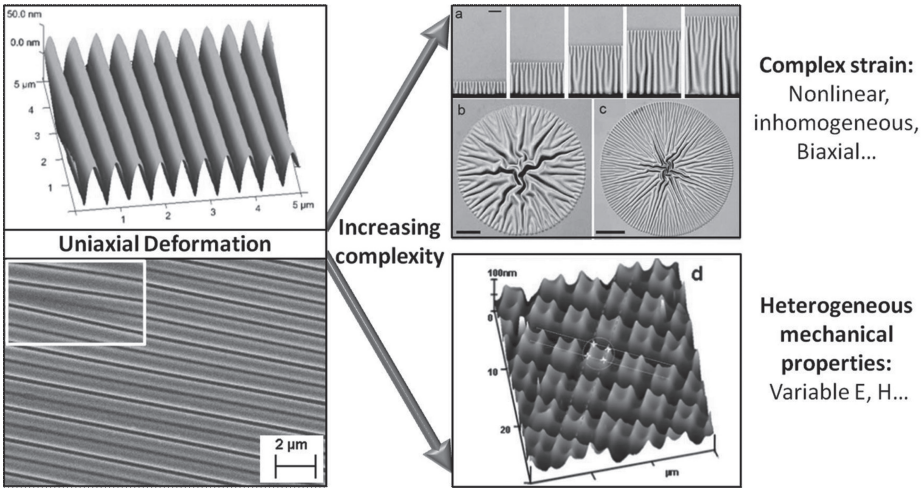


**Figure 9.** 3D AFM and SEM images of a PDMS wrinkled substrate. Inset on SEM image shows "Y"-type junction on wrinkles (left). Wrinkles with complex structures (right). Adapted with permission.[137] Copyright 2010, The Royal Society of Chemistry. Adapted with permission.[179] Copyright 2012, The Royal Society of Chemistry. Adapted with permission.[182] Copyright 2010, The Royal Society of Chemistry.

promising systems to realize complex, hierarchical surface patterns and will stay within the focus of researchers. Several recent developments on this field have been already achieved and can be grouped in two main classes, as shown in **Figure 9**. One strategy is to apply more complex strain situations than uni-axial deformation within linear elastic regime. Larger strains can lead to nonlinear effects, complex strain situations can result in hierarchical wrinkle formation, as indicated in Figure 9 top right. The other possibility is to use simple deformation situations, but use mechanically heterogeneous substrates like patterned substrates or substrates which display gradients in film thickness or elastic constants, as indicated in Figure 9, bottom left.

Several examples illustrate typical approaches for complex strain situations. Application of a thin layer of PS and wrinkling can alternatively realized in one step by floating a thin PS layer on a water bath and submerge an elastomeric substrate, with one edge of the film attached to the substrate at the vapor-liquid-substrate contact line.[184] The formation of wrinkles is caused by the deformation of the elastic substrate at the contact line due to the acting capillary forces which cannot be relaxed after film application. This process results in surface wrinkles with tunable wavelength where submerging velocity is the controlling parameter. To induce another distinct wrinkle wavelength perpendicular to the first wrinkle direction resulting in highly complex surface patterns the substrates are compressed in 90° to the wrinkle patterns.[181] Damman and co-workers[182] studied the formation of hierarchical wrinkles prepared via spontaneous wrinkling of a rigid layer (titania) on top of a soft substrate (PS) induced by solvent diffusion. The resulting wrinkled surface patterns show hierarchal wrinkle properties such as wavelength and amplitude. They were able to prepare radial and linear surface patterns via exposure of the layered substrate to vapor. The observed wavefront proceeds due to solvent diffusion and the initial wavelength is constant. With time the wrinkle wavelength increases and "mature" wrinkles are formed. The wavelength evolution was found to follow a power law. This interesting behavior can be explained by taking into account bending of the top layer, viscous flow in the low molecular weight polymer and solvent diffusion. Recently, the same group reported on multiple length scale elastic instabilities.[185] An interesting expansion is the step towards nonplanar substrates. Trindade and co-workers[180] prepared Janus particles with a wrinkled half sphere via selective UV oxidation of one side of urethane/urea polymer micro- and millimeter sized particles. UV-irradiation lead to the formation of a thin rigid film selectively on one hemisphere. After film formation particles were swelled in an appropriate solvent to induce wrinkling. After solvent removal, wrinkles with two dimensions were obtained on one hemisphere.

On the other hand, several examples illustrating the use of patterned substrates/gradient substrates can be found in recent literature. Lu et al.[179] reported on an approach to build up well-defined highly complex surface patterns. A wrinkled surface prepared via plasma oxidation was used to template wrinkle formation on a substrate covered with a thin PS layer based on thermally expansion. Dependent on wrinkle wavelength of the applied template, a second wrinkle hierarchy was introduced to the PS layer. Repeating the templating step with a varied template to substrate angle, lead to highly complex surface patterns with two deep trenches caused by the template and two trenches with smaller depth, caused by the PS film wrinkling so the resulting structure shows four pins.

Watanabe et al.[177] prepared well-ordered checkerboard patterns with a multiple step approach. Basically a PDMS substrate was wrapped around a pipe to apply a mechanical stress. In a second step a thin PMMA layer was applied and swelled in a solvent vapor to introduce a second hierarchy. After stress relaxation well defined checkerboard patterns were formed.

Furthermore, Hanske and co-workers used a combined approach of chemical patterning and template assisted in combination with microcontact printing to organize nanoparticles in complex structures achieving a selective adsorption of particle lines in concrete regions of the substrate. This technique leads not only to linear assemblies, but also to grid like structures.[186]

Gradients in film thickness were first introduced by Stafford and co-workers in wrinkling metrology.[117] Recently, this principle was used in particle assembly by Hiltl and co-workers.[143] Gradients in elastic constants of the substrate were introduced by Claussen and co-workers.[187]

## 4. Conclusions and Outlook

Bioinspiration aids creative research in materials: biological examples have emboldened researchers to design and test new surface microstructures and to look for alternative fabrication processes. Bioinspired versions of the Lotus leaf or the Gecko's adhesion pads motivated systematic basic research into the exact origins of their functions.

Colloidal particles form an interesting basis for bioinspired processes and structures. Artificial particles are sufficiently well understood and robust to employ them in material synthesis. They are easier to observe and analyze than softer objects such as proteins. They are also more familiar to industry. Processes that employ particles are therefore realistic candidates for actual production processes.

Today, particle-based biomimetic material structuring is in its infancy. Even the most advanced of the processes described above are far less complex and controlled than standard processes in semiconductor manufacturing. Even the most complex surface microstructures fabricated from particles are simple compared to structures that occur in simple organisms. We only begin to understand the roles of hierarchy and internal textures of biological structures.

It also remains to be seen which biomimetic processes can successfully be scaled to areas that are required for production. Materials such as emulsion-based photographic film and or, more recently, E-Ink-displays are encouraging examples of large-scale soft processing. Research into the scale-up of biomimetic surface structures is now ongoing worldwide. In the future, biomimetically microstructured, functional surfaces could become standard products that can be integrated with printing processes, roll-to-roll manufacturing and flexible electronics, for example.

## Acknowledgements

The authors thank Professor Dr. Eduard Arzt for his continuing support of the project. Funding from the German Science Foundation (DFG) in the framework of priority programme 1420 and German Research foundation within the collaborative research center SFB 840, as well as funding from the European Research Council (ERC-2012-StG 306686 METAMECH) are gratefully acknowledged.

Received: December 31, 2012
Revised: March 27, 2013
Published online: June 5, 2013

[1] C. Sun, L. Q. Ge, Z. Z. Gu, *Thin Solid Films* **2007**, *515*, 4686.
[2] H. J. Tsai, Y. L. Lee, *Langmuir* **2007**, *23*, 12687.
[3] Y. H. Xiu, L. B. Zhu, D. W. Hess, C. P. Wong, *Langmuir* **2006**, *22*, 9676.
[4] F. C. Cebeci, Z. Z. Wu, L. Zhai, R. E. Cohen, M. F. Rubner, *Langmuir* **2006**, *22*, 2856.
[5] Y. Li, T. Sasaki, Y. Shimizu, N. Koshizaki, *J. Am. Chem. Soc.* **2008**, *130*, 14755.
[6] X. M. Zhang, J. H. Zhang, Z. Y. Ren, X. Li, X. Zhang, D. F. Zhu, T. Q. Wang, T. Tian, B. Yang, *Langmuir* **2009**, *25*, 7375.
[7] P. Kumnorkaew, Y. K. Ee, N. Tansu, J. F. Gilchrist, *Langmuir* **2008**, *24*, 12150.
[8] J. Grandidier, D. M. Callahan, J. N. Munday, H. A. Atwater, *Adv. Mater.* **2011**, *23*, 1272.
[9] M. Madou, *Fundamentals of Microfabrication: The Science of Miniturization*, Taylor & Francis Ltd., New York, **2011**.
[10] C. B. Murray, C. R. Kagan, M. G. Bawendi, *Annu. Rev. Mater. Sci* **2000**, *30*, 545.
[11] H. Kawaguchi, *Prog. Polym. Sci.* **2000**, *25*, 1171.
[12] G. Frens, *Nature Physical Science* **1973**, *241*, 20.
[13] N. Zheng, J. Fan, G. D. Stucky, *J. Am. Chem. Soc.* **2006**, *128*, 6550.
[14] W. Stöber, A. Fink, E. Bohn, *J. Colloid Interface Sci.* **1968**, *26*, 62.
[15] K. D. Hartlen, A. P. T. Athanasopoulos, V. Kitaev, *Langmuir* **2008**, *24*, 1714.
[16] W. L. Min, B. Jiang, P. Jiang, *Adv. Mater.* **2008**, *20*, 3914.
[17] Y. Wang, N. Lu, H. Xu, G. Shi, M. Xu, X. Lin, H. Li, W. Wang, D. Qi, Y. Lu, L. Chi, *Nano Res.* **2010**, *3*, 520.
[18] Y. Li, J. Zhang, B. Yang, *Nano Today* **2010**, *5*, 117.
[19] C.-H. Sun, P. Jiang, B. Jiang, *Appl. Phys. Lett.* **2008**, 92.
[20] K. Liu, L. Jiang, *Annu. Rev. Mater. Res.* **2012**, *42*, 231.
[21] W.-L. Min, B. Jiang, P. Jiang, *Adv. Mater.* **2008**, *20*, 3914.
[22] Y. Lu, G. L. Liu, J. Kim, Y. X. Mejia, L. P. Lee, *Nano Lett.* **2005**, *5*, 119.
[23] C. Werdinius, L. Österlund, B. Kasemo, *Langmuir* **2003**, *19*, 458.
[24] B. Wickman, Y. E. Seidel, Z. Jusys, B. Kasemo, R. J. Behm, *ACS Nano* **2011**, *5*, 2547.
[25] M. A. Wood, *J. R. Soc. Interface* **2007**, *4*, 1.
[26] Z. P. Huang, H. Fang, J. Zhu, *Adv. Mater.* **2007**, *19*, 744.
[27] A. Vlad, A. Frölich, T. Zebrowski, C. A. Dutu, K. Busch, S. Melinte, M. Wegener, I. Huynen, *Adv. Funct. Mater.* **2013**, *23*, 1164.
[28] B. G. Jung, S.-H. Min, C.-W. Kwon, S.-H. Park, K.-B. Kim, T.-S. Yoon, *J. Electrochem. Soc.* **2009**, *156*, 86.
[29] J. Perlich, M. Schwartzkopf, V. Körstgens, D. Erb, J. F. H. Risch, P. M.-Buschbaum, R. Röhlsberger, S. V. Roth, R. Gehrke, *Phys. Status Solidi* **2012**, *6*, 253.
[30] D. Wang, H. Möhwald, *Adv. Mater.* **2004**, *16*, 244.
[31] J. C. Hulteen, R. P. v. Duyne, *J. Vac. Sci. Technol. A* **1995**, *13*, 1553.
[32] M. Trau, S. Sankaran, D. A. Saville, I. A. Aksay, *Nature* **1995**, *374*, 437.
[33] A. E. Larsen, D. G. Grier, *Phys. Rev. Lett.* **1996**, *76*, 3862.
[34] A. Kosiorek, W. Kandulski, P. Chudzinski, K. Kempa, M. Giersig, *Nano Lett.* **2004**, *4*, 1359.
[35] N. Vogel, S. Goerres, K. Landfester, C. K. Weiss, *Macromol. Chem. Phys.* **2011**, *212*, 1719.
[36] Y. Lin, H. Skaff, T. Emrick, A. D. Dinsmore, T. P. Russell, *Science* **2003**, *299*, 226.
[37] N. D. Denkov, D. Velev, P. A. Kralchevsky, I. B. Ivanov, H. Yoshimura, K. Nagayama, *Langmuir* **1992**, *8*, 3183.
[38] B. G. Prevo, O. D. Velev, *Langmuir* **2004**, *20*, 2099.
[39] L. Malaquin, T. Kraus, H. Schmid, E. Delamarche, H. Wolf, *Langmuir* **2007**, *23*, 11513.
[40] P. Born, S. Blum, A. Munoz, T. Kraus, *Langmuir* **2011**, *27*, 8621.
[41] K. Kempa, B. Kimball, J. Rybczynski, Z. P. Huang, P. F. Wu, D. Steeves, M. Sennett, M. Giersig, D. V. G. L. N. Rao,

D. L. Carnahan, D. Z. Wang, J. Y. Lao, W. Z. Li, Z. F. Ren, *Nano Lett.* **2003**, *3*, 13.
[42] F. Mesequer, R. Fenollosa, *J. Mater. Chem.* **2005**, *15*, 4577.
[43] C. Haginoya, M. Ishibashi, K. Koike, *Appl. Phys. Lett.* **1997**, 71.
[44] D.-G. Choi, H. K. Yu, S. G. Jang, S.-M. Yang, *J. Am Chem. Soc.* **2004**, *126*, 7019.
[45] C. Cong, W. C. Junus, Z. Shen, T. Yu, *Nanoscale Res. Lett.* **2009**, *4*, 1324.
[46] A. Plettl, F. Enderle, M. Saitner, A. Manzke, C. Pfahler, S. Wiedemann, P. Ziemann, *Adv. Funct. Mater.* **2009**, *19*, 3279.
[47] Y. Li, E. J. Lee, W. Cai, K. Y. Kim, S. O. Cho, *ACS Nano* **2008**, *2*, 1108.
[48] A. Manzke, N. Vogel, C. K. Weiss, U. Ziener, A. Plettl, K. Landfester, P. Ziemann, *Nanoscale* **2011**, *3*, 2523.
[49] M. Karg, S. Jaber, T. Hellweg, P. Mulvaney, *Langmuir* **2011**, *27*, 820.
[50] D. Brodoceanu, C. Fang, N. H. Voelcker, C. T. Bauer, A. Wonn, E. Kroner, E. Arzt, T. Krauss, *Nanotechnology* **2013**, *24*, 085304.
[51] L. Isa, K. Kumar, M. Müller, J. Grolig, M. Textor, E. Reimhult, *ACS Nano* **2010**, *4*, 5665.
[52] A. Palla-Papavlu, V. Dinca, I. Paraico, A. Moldovan, J. Shaw-Stewart, C. W. Schneider, E. Kovacs, T. Lippert, M. Dinescu, *J. Appl. Phys.* **2010**, *108*, 033111.
[53] T. Kraus, L. Malaquin, H. Schmid, W. Riess, N. D. Spencer, H. Wolf, *Nat. Nanotechnol.* **2007**, *2*, 570.
[54] Z. Huang, N. Geyer, P. Werner, J. de Boor, U. Gösele, *Adv. Mater.* **2011**, *23*, 285.
[55] H. Asoh, A. Oide, S. Ono, *Electrochem. Commun.* **2006**, *8*, 1817.
[56] C. W. Blackledge, J. M. Szarko, A. Dupont, G. H. Chan, E. L. Read, S. R. Leone, *J. Nanosci. Nanotechnol.* **2007**, *7*, 3336.
[57] S. V. Kesapragada, D. Gall, *Thin Solid Films* **2006**, *494*, 234.
[58] J. Y. Chen, W.-L. Chang, C. K. Huang, K. W. Sun, *Opt. Express* **2011**, *19*, 14411.
[59] A. Kosiorek, W. Kandulski, H. Glaczynska, M. Giersig, *Small* **2005**, *1*, 439.
[60] Y. Li, W. Cai, B. Cao, G. Duan, F. Sun, *Polymer* **2005**, *46*, 12033.
[61] X. D. Wang, E. Graugnard, J. S. King, Z. L. Wang, C. J. Summers, *Nano Lett.* **2004**, *4*, 2223.
[62] H. Hassanin, A. Mohammadkhani, K. Jiang, *Lab Chip* **2012**, *12*, 4160.
[63] H. K. Choy, M. H. Kim, S. H. Im, O. O. Park, *Adv. Funct. Mater.* **2009**, *19*, 1594.
[64] Y. Li, J. Zhang, S. Zhu, H. Dong, F. Jia, Z. Wang, Z. Sun, L. Zhang, Y. Li, H. Li, W. Xu, B. Yang, *Adv. Mater.* **2009**, *21*, 4731.
[65] P.-S. Tsai, Y.-M. Yang, Y.-L. Lee, *Nanotechnology* **2007**,*18,* 465604.
[66] W. Ming, D. Wu, R. van Benthem, G. d. With, *Nano Lett.* **2005**, *5*, 2298.
[67] J. Zhu, C.-M. Hsu, Z. Yu, S. Fan, Y. Cui, *Nano Lett.* **2010**, *10*, 1979.
[68] Z.-Z. Gu, H. Uetsuka, K. Takahashi, R. Nakajima, H. Onishi, A. Fujishima, O. Sato, *Angew. Chem. Int. Ed.* **2003**, *42*, 894.
[69] A. Solga, Z. Cerman, B. F. Striffler, M. Spaeth, W. Barthlott, *Bioinsp. Biomim.* **2007**, *2*, S126.
[70] L. Feng, S. Li, Y. Li, H. Li, L. Zhang, J. Zhai, Y. Song, B. Liu, L. Jiang, D. Zhu, *Adv. Mater.* **2002**, *14*, 1857.
[71] Z. Guo, W. Liu, B.-L. Su, *J. Colloid Interface Sci.* **2011**, *353*, 335.
[72] C.-H. Xue, S.-T. Jia, J. Zhang, J.-Z. Ma, *Sci. Technol. Adv. Mater.* **2010**, *11*.
[73] A. N. Shipway, E. Katz, I. Willner, *ChemPhysChem* **2000**, *1*, 18.
[74] O. D. Velev, S. Gupta, *Adv. Mater.* **2009**, *21*, 1897.
[75] J. H. Zhang, Y. F. Li, X. M. Zhang, B. Yang, *Adv. Mater.* **2010**, *22*, 4249.
[76] F. Li, D. P. Josephson, A. Stein, *Angew. Chem. Int. Ed.* **2011**, *50*, 360.
[77] E. Duguet, A. Desert, A. Perro, S. Ravaine, *Chem. Soc. Rev.* **2011**, *40*, 941.
[78] C. A. Fustin, G. Glasser, H. W. Spiess, U. Jonas, *Langmuir* **2004**, *20*, 9114.
[79] W. M. Choi, O. O. Park, *Colloid Surf., A* **2006**, *277*, 131.
[80] J. Aizenberg, P. V. Braun, P. Wiltzius, *Phys. Rev. Lett.* **2000**, *84*, 2997.
[81] N. N. Khanh, K. B. Yoon, *J. Am Chem. Soc.* **2009**, *131*, 14228.
[82] J. P. Hoogenboom, C. Retif, E. de Bres, M. V. de Boer, A. K. van Langen-Suurling, J. Romijn, A. van Blaaderen, *Nano Lett.* **2004**, *4*, 205.
[83] N. V. Dziomkina, M. A. Hempenius, G. J. Vancso, *Colloid Surf., A* **2009**, *342*, 8.
[84] H. K. Choi, S. H. Im, O. O. Park, *Langmuir* **2010**, *26*, 12500.
[85] Y. D. Yin, Y. Lu, B. Gates, Y. Xia, *J. Am. Chem. Soc.* **2001**, *123*, 8718.
[86] J. Seo, H. Lee, S. Lee, T. I. Lee, J. M. Myoung, T. Lee, *Small* **2012**, *8*, 1614.
[87] Y. H. Kim, J. Park, P. J. Yoo, P. T. Hammond, *Adv. Mater.* **2007**, *19*, 4426.
[88] D. Y. Xia, A. Biswas, D. Li, S. R. J. Brueck, *Adv. Mater.* **2004**, *16*, 1427.
[89] Y. N. Xia, Y. D. Yin, Y. Lu, J. McLellan, *Adv. Funct. Mater.* **2003**, *13*, 907.
[90] D. Solis, B. Willingham, S. L. Nauert, L. S. Slaughter, J. Olson, P. Swanglap, A. Paul, W.-S. Chang, S. Link, *Nano Lett.* **2012**, *12*, 1349.
[91] A. van Blaaderen, R. Ruel, P. Wiltzius, *Nature* **1997**, *385*, 321.
[92] K. H. Lin, J. C. Crocker, V. Prasad, A. Schofield, D. A. Weitz, T. C. Lubensky, A. G. Yodh, *Phys. Rev. Lett.* **2000**, *85*, 1770.
[93] E. Kim, Y. N. Xia, G. M. Whitesides, *Adv. Mater.* **1996**, *8*, 245.
[94] S. M. Yang, G. A. Ozin, *Chem. Commun.* **2000**, 2507.
[95] J. Tien, A. Terfort, G. M. Whitesides, *Langmuir* **1997**, *13*, 5349.
[96] G. O'Sullivan, D. Kilbane, R. D'Arcy, *J. Mod. Opt.* **2012**, *59*, 855.
[97] D. Bratton, D. Yang, J. Y. Dai, C. K. Ober, *Polym. Adv. Technol.* **2006**, *17*, 94.
[98] A. E. Grigorescu, C. W. Hagen, *Nanotechnology* **2009**, 20.
[99] S. Matsui, Y. Ochiai, *Nanotechnology* **1996**, *7*, 247.
[100] J. Genzer, J. Groenewold, *Soft Matter* **2006**, *2*, 310.
[101] N. Bowden, S. Brittain, A. G. Evans, J. W. Hutchinson, G. M. Whitesides, *Nature* **1998**, *393*, 146.
[102] W. T. S. Huck, N. Bowden, P. Onck, T. Pardoen, J. W. Hutchinson, G. M. Whitesides, *Langmuir* **2000**, *16*, 3497.
[103] A. Vaziri, *Soft Matter* **2010**, *6*, 5647.
[104] J. Groenewold, *Physica A* **2001**, *298*, 32.
[105] E. Cerda, K. Ravi-Chandar, L. Mahadevan, *Nature* **2002**, *419*, 579.
[106] A. Schweikart, A. Fery, *Microchim. Acta* **2009**, *165*, 249.
[107] M. A. Biot, *Proc. R. Soc. London, Ser. A* **1957**, *242*, 444.
[108] M. A. Biot, *Mechanics of Incremental Deformations*, John Wiley & Sons, Inc., New York **1965.**
[109] L. D. Landau, E. M. Lifshitz, *Theory of Elasticity*, Nauka, Moscow **1965**.
[110] A. L. Volynskii, S. Bazhenov, O. V. Lebedeva, N. F. Bakeev, *J. Mater. Sci.* **2000**, *35*, 547
[111] R. Huang, *J. Mech. Phys. Solids* **2005**, *53*, 63.
[112] H. Jiang, D.-Y. Khang, J. Song, Y. Sun, Y. Huang, J. A. Rogers, *Proc. Natl. Acad. Sci. USA* **2007**, *104*, 15607.
[113] A. J. Nolte, R. E. Cohen, M. F. Rubner, *Macromolecules* **2006**, *39*, 4841
[114] E. A. Wilder, S. Guo, S. Lin-Gibson, M. J. Fasolka, C. M. Stafford, *Macromolecules* **2006**, *39*, 4138.
[115] C. Harrison, C. M. Stafford, W. Zhang, A. Karim, *Appl. Phys. Lett.* **2004**, *85*, 4016.
[116] T. Okayasu, H.-L. Zhang, D. G. Bucknall, G. A. D. Briggs, *Adv. Funct. Mater.* **2004**, *14*, 1081.
[117] C. M. Stafford, C. Harrison, K. L. Beers, A. Karim, E. J. Amis, M. R. Vanlandingham, H. C. Kim, W. Volksen, R. D. Miller, E. E. Simonyi, *Nat. Mater.* **2004**, *3*, 545.
[118] H. Huang, J. Y. Chung, A. J. Nolte, C. M. Stafford, *Chem. Mater.* **2007**, *19*, 6555.

[119] N. Bowden, W. T. S. Huck, K. E. Paul, G. M. Whitesides, *Appl. Phys. Lett.* **1999**, *75*, 2557.
[120] K. Efimenko, W. E. Wallace, J. Genzer, *J. Colloid Interface Sci.* **2002**, *254*, 306.
[121] M. Watanabe, K. Mizukami, *Macromolecules* **2012**, *45*, 7128.
[122] E. Cerda, L. Mahadevan, *Phys. Rev. Lett.* **2003**, *90*, 074302.
[123] A. Schweikart, N. Pazos-Perez, R. A. Alvarez-Puebla, A. Fery, *Soft Matter* **2011**, *7*, 4093.
[124] S. Cai, D. Breid, A. J. Crosby, Z. Suo, J. W. Hutchinson, *J. Mech. Phys. Solids* **2011**, *59*, 1094.
[125] A. Schweikart, D. Zimin, U. A. Handge, M. Bennemann, V. Altstädt, A. Fery, K. Koch, *Macromol. Chem. Phys.* **2010**, *211*, 259.
[126] S. Park, A. Böker, *J. Mater. Chem.* **2011**, *21*, 11734.
[127] K. Efimenko, M. Rackaitis, E. Manias, A. Vaziri, L. Mahadevan, J. Genzer, *Nat. Mater.* **2005**, *4*, 293.
[128] Y. Xuan, X. Guo, Y. Cui, C. Yuan, H. Ge, B. Cui, Y. Chen, *Soft Matter* **2012**, *8*, 9603.
[129] J. Charles, *Soft Matter* **2008**, *4*, 1805.
[130] H.-N. Kim, S.-H. Lee, K.-Y. Suh, *Lab Chip* **2011**, *11*, 717.
[131] Y. Ni, D. Yang, L. He, *Phys. Rev. E* **2012**, *86*, 031604.
[132] W. H. Koo, S. M. Jeong, F. Araoka, K. Ishikawa, S. Nishimura, T. Toyooka, H. Takezoe, *Nat. Photonics* **2010**, *4*, 222.
[133] S. Vajpayee, K. Khare, S. Yang, C.-Y. Hui, A. Jagota, *Adv. Funct. Mater.* **2011**, *21*, 547.
[134] C.-M. Chen, S. Yang, *Polym. Int.* **2012**, *61*, 1041.
[135] S. John, *Phys. Rev. Lett.* **1987**, *58*, 2486.
[136] E. Yablonovitch, *Phys. Rev. Lett.* **1987**, *58*, 2059.
[137] N. Pazos-Perez, W. H. Ni, A. Schweikart, R. A. Alvarez-Puebla, A. Fery, L. M. Liz-Marzan, *Chem. Sci.* **2010**, *1*, 174.
[138] M. K. Gupta, S. Chang, S. Singamaneni, L. F. Drummy, R. Gunawidjaja, R. R. Naik, V. V. Tsukruk, *Small* **2011**, *7*, 1192.
[139] C. Lu, H. Möhwald, A. Fery, *Soft Matter* **2007**, *3*, 1530.
[140] D. C. Hyun, G. D. Moon, E. C. Cho, U. Jeong, *Adv. Funct. Mater.* **2009**, *19*, 2155.
[141] A. Horn, S. Hiltl, A. Fery, A. Boeker, *Small* **2010**, *6*, 2122.
[142] S. Hiltl, M.-P. Schuerings, A. Balaceanu, V. Mayorga, C. Liedel, A. Pich, A. Boeker, *Soft Matter* **2011**, *7*, 8231.
[143] S. Hiltl, J. Oltmanns, A. Boker, *Nanoscale* **2012**, *4*, 7338.
[144] A. Schweikart, A. Fortini, A. Wittemann, M. Schmidt, A. Fery, *Soft Matter* **2010**, *6*, 5860.
[145] M. Müller, M. Karg, A. Fortini, T. Hellweg, A. Fery, *Nanoscale* **2012**, *4*, 2491.
[146] M. Müller, M. Tebbe, D. V. Andreeva, M. Karg, A. Alvarez Puebla Ramon, N. Pazos-Perez, A. Fery, *Langmuir* **2012**, *28*, 9168.
[147] M. Pretzl, A. Schweikart, C. Hanske, A. Chiche, U. Zettl, A. Horn, A. Böker, A. Fery, *Langmuir* **2008**, *24*, 12748.
[148] C. Badre, J. P. Chapel, S. Yang, *Soft Matter* **2011**, *7*, 9886.
[149] K. Efimenko, J. Finlay, M. E. Callow, J. A. Callow, J. Genzer, *ACS Appl. Mater. Interfaces* **2009**, *1*, 1031.
[150] R. A. Alvarez-Puebla, L. M. Liz-Marzan, *Energ. Environ. Sci.* **2010**, *3*, 1011.
[151] H. A. Atwater, A. Polman, *Nat. Mater.* **2010**, *9*, 865.
[152] J. M. Baik, M. Zielke, M. H. Kim, K. L. Turner, A. M. Wodtke, M. Moskovits, *ACS Nano* **2010**, *4*, 3117.
[153] N. Engheta, *Science* **2007**, *317*, 1698.
[154] S. H. Ko, I. Park, H. Pan, C. P. Grigoropoulos, A. P. Pisano, C. K. Luscombe, J. M. J. Frechet, *Nano Lett.* **2007**, *7*, 1869.
[155] S. J. Koh, *Nanoscale Res. Lett.* **2007**, *2*, 519.
[156] S. Mitragotri, J. Lahann, *Nat. Mater.* **2009**, *8*, 15.
[157] J. A. Schuller, E. S. Barnard, W. S. Cai, Y. C. Jun, J. S. White, M. L. Brongersma, *Nat. Mater.* **2010**, *9*, 193.
[158] Z. Q. Sun, B. Yang, *Nanoscale Res. Lett.* **2006**, *1*, 46.
[159] Y. H. Wang, C. A. Mirkin, S. J. Park, *ACS Nano* **2009**, *3*, 1049.
[160] M. Moskovits, *J. Raman Spectrosc.* **2005**, *36*, 485.
[161] L. Brus, *Acc. Chem. Res.* **2008**, *41*, 1742.
[162] G. Braun, I. Pavel, A. R. Morrill, D. S. Seferos, G. C. Bazan, N. O. Reich, M. Moskovits, *J. Am. Chem. Soc.* **2007**, *129*, 7760.
[163] R. Kodiyath, J. Wang, Z. A. Combs, S. Chang, M. K. Gupta, K. D. Anderson, R. J. C. Brown, V. V. Tsukruk, *Small* **2011**, *7*, 3452.
[164] R. Kodiyath, T. A. Papadopoulos, J. Wang, Z. A. Combs, H. Li, R. J. C. Brown, J. L. Bredas, V. V. Tsukruk, *J. Phys. Chem. C* **2012**, *116*, 13917.
[165] H. Ko, S. Singamaneni, V. V. Tsukruk, *Small* **2008**, *4*, 1576.
[166] S. M. Nie, S. R. Emery, *Science* **1997**, *275*, 1102.
[167] K. Kneipp, Y. Wang, H. Kneipp, L. T. Perelman, I. Itzkan, R. Dasari, M. S. Feld, *Phys. Rev. Lett.* **1997**, *78*, 1667.
[168] N. Pazos-Perez, F. J. G. de Abajo, A. Fery, R. A. Alvarez-Puebla, *Langmuir* **2012**, *28*, 8909.
[169] L. Rodriguez-Lorenzo, R. de la Rica, R. A. Alvarez-Puebla, L. M. Liz-Marzan, M. M. Stevens, *Nat. Mater.* **2012**, *11*, 604.
[170] F. Hao, C. L. Nehl, J. H. Hafner, P. Nordlander, *Nano Lett.* **2007**, *7*, 729.
[171] L. Rodriguez-Lorenzo, R. A. Alvarez-Puebla, I. Pastoriza-Santos, S. Mazzucco, O. Stephan, M. Kociak, L. M. Liz-Marzan, F. J. G. de Abajo, *J. Am. Chem. Soc.* **2009**, *131*, 4616.
[172] L. Rodriguez-Lorenzo, R. A. Alvarez-Puebla, F. J. G. de Abajo, L. M. Liz-Marzan, *J. Phys. Chem. C* **2010**, *114*, 7336.
[173] P. Aldeanueva-Potel, E. Carbo-Argibay, N. Pazos-Perez, S. Barbosa, I. Pastoriza-Santos, R. A. Alvarez-Puebla, L. M. Liz-Marzan, *ChemPhysChem* **2012**, *13*, 2561.
[174] X. Chen, J. W. Hutchinson, *J. Appl. Mech.* **2004**, *71*, 597.
[175] P. C. Lin, S. Yang, *Appl. Phys. Lett.* **2007**, *90*, 3.
[176] W. M. Choi, J. Song, D.-Y. Khang, H. Jiang, Y. Y. Huang, J. A. Rogers, *Nano Lett.* **2007**, *7*, 1655.
[177] M. Watanabe, *Soft Matter* **2012**, *8*, 1563.
[178] S. Yang, K. Khare, P.-C. Lin, *Adv. Funct. Mater.* **2010**, *20*, 2550.
[179] J. Yin, C. Lu, *Soft Matter* **2012**, *8*, 6528.
[180] A. C. Trindade, J. P. Canejo, P. Patricio, P. Brogueira, P. I. Teixeira, M. H. Godinho, *J. Mater. Chem.* **2012**, *22*, 22044.
[181] C. S. Davis, A. J. Crosby, *J. Polym. Sci. Pol. Phys.* **2012**, *50*, 1225.
[182] H. Vandeparre, S. Gabriele, F. Brau, C. Gay, K. K. Parkerc, P. Damman, *Soft Matter* **2010**, *6*, 5751.
[183] T. Ohzono, H. Monobe, *Langmuir* **2010**, *26*, 6127.
[184] G. Miquelard-Garnier, A. B. Croll, C. S. Davis, A. J. Crosby, *Soft Matter* **2010**, *6*, 5789.
[185] F. Brau, H. Vandeparre, A. Sabbah, C. Poulard, A. Boudaoud, P. Damman, *Nat. Phys.* **2011**, *7*, 56.
[186] C. Hanske, M. B. Müller, V. Bieber, M. Tebbe, S. Jessl, A. Wittemann, A. Fery, *Langmuir* **2012**, *28*, 16745.
[187] K. U. Claussen, M. Tebbe, R. Giesa, A. Schweikart, A. Fery, H.-W. Schmidt, *RSC Adv.* **2012**,*2*, 10185.
[188] G. M. Zhang, J. Zhang, G. Y. Xie, Z. F. Liu, H. B. Shao, *Small* **2006**, *2*, 1440.
[189] Y. Y. Yan, N. Gao, W. Barthlott, *Adv. Colloid Interface Sci.* **2011**, *169*, 80.
[190] J. Aizenberg, A. Tkachenko, S. Weiner, L. Addadi, G. Hendler, *Nature* **2001**, *412*, 819.
[191] D. G. Stavenga, S. Foletti, G. Palasantzas, K. Arikawa, *Proc. R. Soc. B* **2006**, *273*, 661.
[192] K. Lee, W. Wagermaier, A. Masic, K. P. Kommareddy, M. Bennet, I. Manjubala, S. W. Lee, S. B. Park, H. Colfen, P. Fratzl, *Nat. Commun.* **2012**, *3*, 725.
[193] D. Voigt, A. Schweikart, A. Fery, S. Gorb, *J Exp Biol* **2012**, *215*, 1975.
[194] P. Born, A. Munoz, C. Cavelius, T. Kraus, *Langmuir* **2012**, *28*, 8300.
[195] C. Li, G. S. Hong, P. W. Wang, D. P. Yu, L. M. Qi, *Chem. Mater.* **2009**, *21*, 891.